

Selective excitation of single and multiple quantum transitions for spin $7/2$ in NQR

By S. Z. AGEEV and B. C. SANCTUARY

Department of Chemistry, McGill University, 801 Sherbrooke Street West,
Montreal, PQ, Canada H3A 2K6

(Received 19 June 1995; revised version accepted 5 December 1995)

The dynamics of spin $7/2$ in pure NQR is considered. The orientation of the applied RF field is assumed arbitrary and $\eta \neq 0$. For this situation various selective pulses are considered and analytical results obtained. Shaped pulses are also treated. A key feature of this work is to construct the interaction representation from which an analytical calculation, using the computer program 'Maple', can be obtained in a tractable form. The results presented are general for all half integer spins of magnitude higher than $1/2$.

1. Introduction

NQR has the simplifying advantage that the nuclear electric quadrupolar interaction usually dominates the dipole–dipole interaction. This means that the spin dynamics can be treated, to a good approximation, as an average over a single spin with $2I+1$ states. Pulses and, via internal interactions, developments of spin states can be calculated in a straightforward manner, providing a description from which various physical constants can be extracted, or a framework from which relaxation can be studied.

On the other hand, the study of spin dynamics in NQR causes difficulties. For one, non-zero asymmetry can lead to intractable calculations. Another problem is that the RF field is oriented randomly in powders. Moreover, RF pulses are not 'hard', with the consequence that the quadrupole cannot be ignored while a pulse is on. In NQR, however, methods to handle these difficulties have been developed for spins of low magnitude. In 1977, Pratt led the way by introducing an interaction representation. He found that the response of the quadrupolar spin $3/2$ nuclei is similar to that of a spin $1/2$ NMR [1], thereby enabling a variety of approaches used in NMR to be carried over to NQR.

From a mathematical viewpoint, these approaches have relied on operator formalisms such as fictitious spin $1/2$ [2], spherical tensor [3] and projection operators [4] techniques. However, the algebraic complexity and corresponding lengthy tables of commutation relations is the common drawback of these methods. Obviously calculation involving spins higher than $3/2$ become even more cumbersome, and manual calculations become more error prone. Such approaches also often mask the physical picture of the quadrupolar phenomena in progress. An attempt to clarify the physical picture has been made by Krishnan *et al.* [5], but those arguments are applied only to half integer spins. Moreover, extension to $\eta \neq 0$ is not obvious.

Recently, using simple matrix methods, we have extended spin dynamic calculations for $\eta \neq 0$ cases involving spin $3/2$ and $5/2$ [6, 7]. This is possible due to developments of computer algebra which allow facile manipulation of matrices of

dimension needed for such calculations. Although computer algebra has allowed significant extension so that higher spins can be treated routinely, its use requires some care and strategy. Extension from spin $5/2$ to $7/2$ is not straightforward. Algebraic equations easily can become too long to treat, and proper reduction techniques to obtain matrices of manageable size must be invoked. To this end, it is not surprising that no studies of spin $7/2$ exist in the literature. In this paper we consider this problem and present spin $7/2$ results with $\eta \neq 0$ as it responds to selective RF pulses. In tandem with previous approaches, we assume that the pulses are selective [5] since in NQR the zero magnetic field splittings are unequal, and excite only one specific multiple quantum transition. We also do not restrict the RF field to one direction in space. Consequently, field orientation angles can be averaged over, thereby allowing application to powder samples to follow without difficulties. Finally, we allow for shaped RF pulses which are used in both NMR [8] and NQR [7].

The calculation is performed using the computer program 'Maple' [9]. It is shown here that the excitation of these spin systems can be considered in the interaction picture as being equivalent to the excitation of two uncoupled spins of $1/2$. At any time these spins $1/2$ have equal x and y projections of the magnetization vector whereas their z components are directed oppositely. The main important difference with NMR is the appearance of an effective RF field frequency which depends on the orientation of the crystal with respect to the applied RF field and transition in question. In addition, in this paper we allow an arbitrary non-singular modulation of the applied RF field. It should be noted that double and higher quantum coherences are not detected in a one pulse excitation experiment for $\eta = 0$ as these are forbidden by well known selection rules [10]. These can be analysed by using multiple-pulse sequences developed by Hatanaka *et al.* [11]. In particular, using this technique double quantum transitions have been investigated theoretically for spin $5/2$ [12] and spin $7/2$ [10]. For the case of spin $7/2$ ($\eta \neq 0$) it is shown in this paper that double and triple quantum transitions can be excited by one-pulse experiments, as these can be allowed transitions according to the selection rules obtained.

One shortcoming of our approach is the restriction to selective excitation. Although excitation in NQR is primarily selective, accidental degeneracies (as a function of η) can arise. On the other hand, for particular special cases, when experimentally more than one frequency is excited, our methods can be modified to study such situations. We also impose one major approximation, well justified in practice: we ignore high frequency (non-secular) terms which give corrections of the order of Bloch–Siegert shifts [13].

This work, then, extends previous computer algebra treatments of $1/2$ integral spins from $I = 3/2$ and $5/2$ to $I = 7/2$ with the same level of approximations and accuracy [6].

2. Eigenvalue and eigenfunction problem for spin $7/2$

The quadrupolar Hamiltonian matrix for a spin $7/2$ in the $|IM\rangle$ basis is given by:

$$H_Q = \frac{\hbar e^2 q Q}{84} \times \begin{bmatrix} 21 & 0 & \eta(21)^{1/2} & 0 & 0 & 0 & 0 & 0 \\ 0 & 3 & 0 & \eta(45)^{1/2} & 0 & 0 & 0 & 0 \\ \eta(21)^{1/2} & 0 & -9 & 0 & \eta(60)^{1/2} & 0 & 0 & 0 \\ 0 & \eta(45)^{1/2} & 0 & -15 & 0 & \eta(60)^{1/2} & 0 & 0 \\ 0 & 0 & \eta(60)^{1/2} & 0 & -15 & 0 & \eta(45)^{1/2} & 0 \\ 0 & 0 & 0 & \eta(60)^{1/2} & 0 & -9 & 0 & \eta(21)^{1/2} \\ 0 & 0 & 0 & 0 & \eta(45)^{1/2} & 0 & 3 & 0 \\ 0 & 0 & 0 & 0 & 0 & \eta(21)^{1/2} & 0 & 21 \end{bmatrix}. \quad (1)$$

The eigenvalues are doubly degenerate and the trace of H_Q is zero. Thus the corresponding secular equation is of quartic form

$$E^4 - 126(3 + \eta^2)E^2 - 1728(1 - \eta^2)E + 945(3 + \eta^2)^2 = 0, \quad (2)$$

with the solutions given by [14]:

$$\begin{aligned} E_1 &= (R + D)/2, \\ E_2 &= (R - D)/2, \\ E_3 &= -(R - S)/2, \\ E_4 &= -(R + S)/2. \end{aligned} \quad (3)$$

The various constants are

$$\begin{aligned} D &= \left[\frac{1}{2} \left(X + \frac{Y}{R} \right) - R^2 \right]^{1/2}, \\ S &= \left[\frac{1}{2} \left(X - \frac{Y}{R} \right) - R^2 \right]^{1/2}, \end{aligned} \quad (4)$$

and

$$R = 6^{-1/2} [X + (X^2 + 12Z)^{1/2} \cos(\delta/3)]^{1/2}, \quad (5)$$

where

$$\cos \delta = -[X^3 - 36XZ - 54Y^2]/(X^2 + 12Z)^{3/2}. \quad (6)$$

Here X , Y and Z depend on the interaction parameters as

$$\begin{aligned} X &= 504(3 + \eta^2), \\ Y &= 6912(1 - \eta^2), \\ Z &= 15120(3 + \eta^2)^2. \end{aligned} \quad (7)$$

The energies E_1 , E_2 , E_3 , and E_4 are in units of $(\hbar e^2 q Q)/84$ and are ordered as $E_1 \geq E_2$

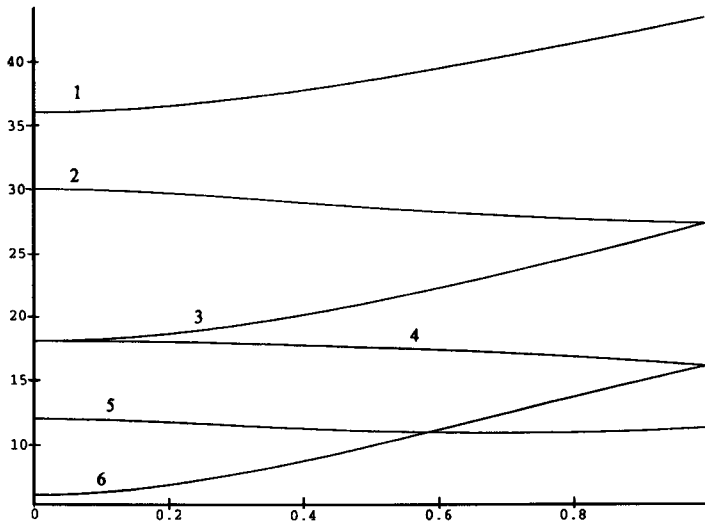


Figure 1. The frequencies of single and multiple quantum transitions ω_Q as functions of η : 1, $\omega_Q = E_1 - E_4$ (triple quantum transition); 2, $\omega_Q = E_1 - E_3$ (double quantum transition); 3, $\omega_Q = E_2 - E_4$ (double quantum transition); 4, $\omega_Q = E_1 - E_2$ (single quantum transition); 5, $\omega_Q = E_2 - E_3$ (single quantum transition); and 6, $\omega_Q = E_3 - E_4$ (single quantum transition).

$\geq E_3 \geq E_4$. In the case of $\eta = 0$ the eigenvalues of Hamiltonian (1) reduce to the simple results $E_1 = 21, E_2 = 3, E_3 = -9, E_4 = -15$. The difficulty with quadrupolar spin 7/2 Hamiltonian (1) is that it is non-diagonal in η . The matrix which diagonalizes quadrupolar spin 7/2 Hamiltonian (1) is given by

$$U = \begin{bmatrix} U_{11} & 0 & U_{13} & 0 & U_{15} & 0 & U_{17} & 0 \\ 0 & U_{22} & 0 & U_{24} & 0 & U_{26} & 0 & U_{28} \\ U_{31} & 0 & U_{33} & 0 & U_{35} & 0 & U_{37} & 0 \\ 0 & U_{42} & 0 & U_{44} & 0 & U_{46} & 0 & U_{48} \\ U_{48} & 0 & U_{46} & 0 & U_{44} & 0 & U_{42} & 0 \\ 0 & U_{37} & 0 & U_{35} & 0 & U_{33} & 0 & U_{31} \\ U_{28} & 0 & U_{26} & 0 & U_{24} & 0 & U_{22} & 0 \\ 0 & U_{17} & 0 & U_{15} & 0 & U_{13} & 0 & U_{11} \end{bmatrix}, \tag{8}$$

where

$$\begin{aligned} U_{11} &= \frac{1}{N_1}, \\ U_{13} &= \frac{1}{N_1} \frac{\eta(21)^{1/2}((15 + E_1)(3 - E_1) + 45\eta^2)}{(E_1 + 9)((15 + E_1)(3 - E_1) + 45\eta^2) + 60\eta^2(E_1 - 3)}, \\ U_{15} &= \frac{1}{N_1} \frac{2\eta^2(315)^{1/2}(3 - E_1)}{(E_1 + 9)((15 + E_1)(3 - E_1) + 45\eta^2) + 60\eta^2(E_1 - 3)}, \\ U_{17} &= -\frac{1}{N_1} \frac{2\eta^3(14175)^{1/2}}{(E_1 + 9)((15 + E_1)(3 - E_1) + 45\eta^2) + 60\eta^2(E_1 - 3)}, \end{aligned} \tag{9}$$

$$\begin{aligned}
 U_{22} &= \frac{1}{N_2}, \\
 U_{24} &= \frac{1}{N_2} \frac{\eta(45)^{1/2}((9+E_2)(E_2-21)-21\eta^2)}{(15+E_2)((9+E_2)(E_2-21)-21\eta^2)+60\eta^2(21-E_2)}, \\
 U_{26} &= \frac{1}{N_2} \frac{(E_2-21)\eta^2(2700)^{1/2}}{(15+E_2)((9+E_2)(E_2-21)-21\eta^2)+60\eta^2(21-E_2)}, \\
 U_{28} &= \frac{1}{N_2} \frac{2\eta^3(14175)^{1/2}}{(15+E_2)((9+E_2)(E_2-21)-21\eta^2)+60\eta^2(21-E_2)}, \tag{10}
 \end{aligned}$$

$$U_{31} = \frac{1}{N_3} \frac{\eta(21)^{1/2}}{E_3-21},$$

$$U_{33} = \frac{1}{N_3},$$

$$U_{35} = \frac{1}{N_3} \frac{\eta(60)^{1/2}(3-E_3)}{(15+E_3)(3-E_3)+45\eta^2},$$

$$U_{37} = -\frac{1}{N_3} \frac{\eta^2(2700)^{1/2}}{(15+E_3)(3-E_3)+45\eta^2}, \tag{11}$$

$$U_{42} = \frac{1}{N_4} \frac{\eta(45)^{1/2}}{E_4-3},$$

$$U_{44} = \frac{1}{N_4},$$

$$U_{46} = \frac{1}{N_4} \frac{\eta(60)^{1/2}(21-E_4)}{(9+E_4)(21-E_4)+21\eta^2},$$

$$U_{48} = -\frac{1}{N_4} \frac{2\eta^2(315)^{1/2}}{(9+E_4)(21-E_4)+21\eta^2}. \tag{12}$$

The constants N_1 , N_2 , N_3 and N_4 are chosen by normalizing each row of the \mathbf{U} matrix to unity. For $\eta = 0$, \mathbf{U} reduces to the identity.

As an example, the doubly degenerate eigenvalue E_1 has eigenfunctions

$$|\pm 1\rangle = U_{11} \left| \frac{7}{2}, \pm \frac{7}{2} \right\rangle + U_{13} \left| \frac{7}{2}, \pm \frac{3}{2} \right\rangle + U_{15} \left| \frac{7}{2}, \mp \frac{1}{2} \right\rangle + U_{17} \left| \frac{7}{2}, \mp \frac{5}{2} \right\rangle. \tag{13}$$

These eigenfunctions are denoted by $|\pm 1\rangle$. The upper signs in equation (13) refer to $|+1\rangle$ and the lower signs refer to $|-1\rangle$. For the eigenvalues E_2 , E_3 and E_4 we similarly define the eigenfunctions of the quadrupolar Hamiltonian as $|\pm 2\rangle$, $|\pm 3\rangle$ and $|\pm 4\rangle$.

3. Effect of RF pulses

The RF Hamiltonian is given by

$$\mathbf{H}_{\text{RF}} = -2\hbar\omega_1 \cos(\omega t - \phi) \mathbf{I} \cdot \mathbf{n}, \tag{14}$$

where the strength ω_1 , the carrier frequency ω , and the phase ϕ , describe the pulse. The

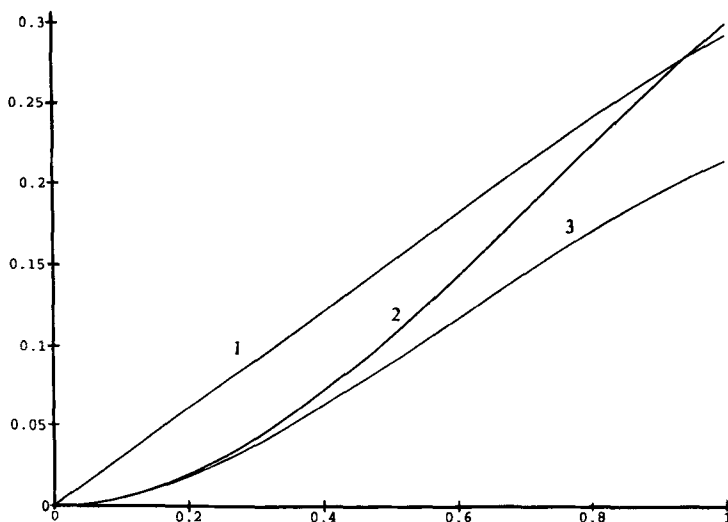


Figure 2. The values a_+ , a_- and e as functions of η for the double quantum transition $|\pm 3\rangle \rightarrow |\pm 1\rangle$: 1, $-a_+$; 2, $-a_-$; and 3, $-e$.

unit vector $\mathbf{n} = (\sin \theta_L \cos \phi_L, \sin \theta_L \sin \phi_L, \cos \theta_L)$ specifies the orientation of the RF coil with respect to the quadrupolar principal axis system (QPAS). We assume that ω_1 and ϕ are non-singular functions of time. The selection rules for spin 7/2 quadrupolar system are deduced by transforming the RF Hamiltonian of equation (14) into the representation where static (quadrupolar) Hamiltonian (1) is diagonal. These transformations are performed easily using Maple. The matrix elements of the angular momentum components in this new frame are lengthy and only the elements of interest with respect to the problem in question are given below.

It should be noted that when $\eta \neq 0$ not only 'single quantum' transitions such as $|\pm 4\rangle \rightarrow |\pm 3\rangle$, $|\pm 3\rangle \rightarrow |\pm 2\rangle$ and $|\pm 2\rangle \rightarrow |\pm 1\rangle$ are allowed but also 'double quantum' $|\pm 4\rangle \rightarrow |\pm 2\rangle$, $|\pm 3\rangle \rightarrow |\pm 1\rangle$ and 'triple quantum' $|\pm 4\rangle \rightarrow |\pm 1\rangle$ transitions are possible. The energy splittings between pairs of degenerate levels of spin 7/2 are in general unequal and a single pulse acts selectively. If the carrier frequency of an RF pulse is close to the frequency of a certain transition, this means that others are off-resonant and are not affected by the pulse. Thus the problem reduces to a study of 4×4 matrices, thereby simplifying the problem considerably. This is an example of the 'simple line' concept when the RF radiation influences exclusively one transition in a spin system of arbitrary complexity [15]. The frequencies of the single and multiple quantum transitions of a spin 7/2 are shown in figure 1 from which it is seen that accidental degeneracies may occur for certain values of η . In particular, when $\eta = 0$ the frequencies of the single quantum $|\pm 2\rangle \rightarrow |\pm 1\rangle$ and double quantum $|\pm 4\rangle \rightarrow |\pm 2\rangle$ transitions are degenerate. However, these cannot be excited simultaneously as the DQ transition in question is forbidden by the selection rule discussed below. For the other cases of degeneracies the treatment given below should be modified.

3.1. Transitions $|\pm 3\rangle \rightarrow |\pm 1\rangle$

Consider, for example the 'double quantum' transition $|\pm 3\rangle \rightarrow |\pm 1\rangle$. The reduced quadrupolar Hamiltonian is given by the diagonal matrix with elements E_1, E_3, E_3 and

E_1 . The reduced RF Hamiltonian in the representation where the quadrupolar Hamiltonian is diagonal is given as

$$\mathbf{H}_{\text{RF}}^r = -2\hbar\omega_1 \cos(\omega t - \phi) \left\{ \sin\theta_L \cos\phi_L \begin{pmatrix} 0 & a_+ & 0 & b_+ \\ a_+ & 0 & c_+ & 0 \\ 0 & c_+ & 0 & a_+ \\ b_+ & 0 & a_+ & 0 \end{pmatrix} \right. \\ \left. + \sin\theta_L \sin\phi_L \begin{pmatrix} 0 & -ia_- & 0 & ib_- \\ ia_- & 0 & -ic_- & 0 \\ 0 & ic_- & 0 & -ia_- \\ -ib_- & 0 & ia_- & 0 \end{pmatrix} \right. \\ \left. + \cos\theta_L \begin{pmatrix} -d & 0 & e & 0 \\ 0 & -d_1 & 0 & -e \\ e & 0 & d_1 & 0 \\ 0 & -e & 0 & d \end{pmatrix} \right\}. \quad (15)$$

In this representation, the rows and columns are in the basis given by $|1\rangle, |-3\rangle, |3\rangle$ and $|-1\rangle$. The constants, $a_{\pm}, b_{\pm}, c_{\pm}, d, d_1$ and e are

$$a_{\pm} = \frac{(7)^{1/2}}{2} U_{11} U_{37} \pm (3)^{1/2} U_{13} U_{37} + \frac{(15)^{1/2}}{2} U_{13} U_{35} \pm 2U_{15} U_{35} + \frac{(15)^{1/2}}{2} U_{33} U_{15} \\ \pm (3)^{1/2} U_{17} U_{33} + \frac{(7)^{1/2}}{2} U_{31} U_{17}, \\ b_{\pm} = \pm (7)^{1/2} U_{11} U_{17} + 2(3)^{1/2} U_{17} U_{13} \pm (15)^{1/2} U_{13} U_{15} + 2U_{15}^2, \\ c_{\pm} = \pm (7)^{1/2} U_{31} U_{37} + 2(3)^{1/2} U_{37} U_{33} \pm (15)^{1/2} U_{33} U_{35} + 2U_{35}^2, \\ d = -\frac{7}{2} U_{11}^2 + \frac{5}{2} U_{17}^2 - \frac{3}{2} U_{13}^2 + \frac{1}{2} U_{15}^2, \\ e = \frac{7}{2} U_{11} U_{31} + \frac{3}{2} U_{13} U_{33} - \frac{1}{2} U_{15} U_{35} - \frac{5}{2} U_{17} U_{37}, \\ d_1 = \frac{7}{2} U_{31}^2 + \frac{3}{2} U_{33}^2 - \frac{2}{35} - \frac{5}{2} U_{37}^2. \quad (16)$$

The interaction picture is introduced by the operator \mathbf{L} as

$$\mathbf{L} = \exp\left(-\frac{1}{2}i\omega t \mathbf{R}\right), \quad (17)$$

where \mathbf{R} is a diagonal matrix with the elements of $(1, -1, -1, 1)$. Transforming the reduced RF Hamiltonian of equation (15) into the interaction frame of equation (17) and discarding high frequency terms [6] gives

$$\tilde{\mathbf{H}}_{\text{RF}}^r = -\frac{\hbar\omega_1}{2} \{\mathbf{P} \cos\phi + \mathbf{Q} \cos\phi\}, \quad (18)$$

with

$$\mathbf{P} = \begin{pmatrix} 0 & \alpha - i\beta & \gamma & 0 \\ \alpha + i\beta & 0 & 0 & -\gamma \\ \gamma & 0 & 0 & \alpha - i\beta \\ 0 & -\gamma & \alpha + i\beta & 0 \end{pmatrix}, \mathbf{Q} = \begin{pmatrix} 0 & -i\alpha - \beta & -i\gamma & 0 \\ i\alpha - \beta & 0 & 0 & -i\gamma \\ i\gamma & 0 & 0 & i\alpha + \beta \\ 0 & i\gamma & -i\alpha + \beta & 0 \end{pmatrix},$$

where

$$\begin{aligned} \alpha &= 2a_+ \sin \theta_L \cos \phi_L, \\ \beta &= 2a_- \sin \theta_L \sin \phi_L, \\ \gamma &= 2e \cos \theta_L. \end{aligned} \tag{19}$$

The values a_+ , a_- and e as functions of η are shown in figure 2.

The reduced quadrupolar Hamiltonian then can be written in a simple diagonal form

$$\mathbf{H}_Q^r = \frac{\hbar\omega_Q}{2} \mathbf{R}, \tag{20}$$

where

$$\omega_Q = \frac{e^2 q Q}{84} (E_1 - E_3) \tag{21}$$

is the actual frequency of the transition and the contribution proportional to the unity matrix is dropped as it resets the energy reference state. The total Hamiltonian in the interaction picture is brought to the block-diagonal form by the unitary transformation \mathbf{T} [7],

$$\mathbf{T} = \begin{pmatrix} \gamma/r & 0 & 0 & (\alpha - i\beta)/r \\ 0 & 0 & 1 & 0 \\ 0 & -1 & 0 & 0 \\ -(\alpha + i\beta)/r & 0 & 0 & \gamma/r \end{pmatrix}, \tag{22}$$

where

$$r = (\alpha^2 + \beta^2 + \gamma^2)^{1/2}, \tag{23}$$

to give

$$\tilde{\mathbf{H}}_T^r = \mathbf{T} \left(\tilde{\mathbf{H}}_{RF}^r + \frac{\hbar(\omega_Q - \omega)}{2} \mathbf{R} \right) \mathbf{T}^+ = \begin{pmatrix} \mathbf{h}_+ & \mathbf{0} \\ \mathbf{0} & \mathbf{h}_- \end{pmatrix}, \tag{24}$$

with

$$\mathbf{h}_\pm = \pm \frac{1}{2} \hbar (\omega_Q - \omega) \begin{pmatrix} 1 & 0 \\ 0 & -1 \end{pmatrix} - \frac{1}{2} \hbar \omega_{1\text{eff}} \begin{pmatrix} 0 & e^{\mp i\phi} \\ e^{\pm i\phi} & 0 \end{pmatrix}$$

where the upper sign refers to h_+ and the lower sign refers to h_- and

$$\omega_{1\text{eff}} = \omega_1 r. \tag{25}$$

It should be noted that the transformation \mathbf{T} does not change the reduced quadrupolar Hamiltonian of equation (20) and the initial reduced density matrix is given by simply

$$\rho(0) = \mathbf{R}. \tag{26}$$

The evolution of the reduced density matrix in the interaction picture is governed by the Liouville equation

$$i\hbar \frac{\partial \tilde{\rho}}{\partial t} = [\tilde{\mathbf{H}}_T^r, \tilde{\rho}]_-. \tag{27}$$

Using equation (24) we arrive at

$$i\hbar \frac{\partial \tilde{\rho}_k}{\partial t} = [\mathbf{h}_k, \tilde{\rho}_k]_-, \tag{28}$$

where

$$\tilde{\rho}(t) = \begin{pmatrix} \rho_+ & \mathbf{0} \\ \mathbf{0} & \rho_- \end{pmatrix},$$

k labels $+$ and $-$, and the initial condition is given by equation (26).

The general solution to equation (28) is

$$\begin{aligned} \tilde{\rho}_+ &= \begin{pmatrix} \sigma_{11} & \sigma_{12} \\ \sigma_{12}^* & -\sigma_{11} \end{pmatrix}, \\ \tilde{\rho}_- &= \begin{pmatrix} -\sigma_{11} & \sigma_{12}^* \\ \sigma_{12} & \sigma_{11} \end{pmatrix}. \end{aligned} \quad (29)$$

Note that $\sigma_{11}^2 + |\sigma_{12}|^2 = 1$.

Introducing $f = \sigma_{12}^*/(1 + \sigma_{11})$ to transform equation (28) with $k = +$ into a Riccati equation [8],

$$\dot{f} - i\Delta\omega f + \frac{1}{2}i\Omega^*(t)f^2 - \frac{1}{2}i\Omega(t) = 0, \quad (30)$$

where $\Omega(t) = \omega_{\text{1eff}} e^{i\phi}$ and $\Delta\omega = \omega_Q - \omega$.

Equation (29) can be also written in terms of Euler angles, α_1 , β_1 and γ_1 , using the rotation operator approach [6, 16] and writing

$$T \exp\left(-\frac{i}{\hbar} \int_0^t \mathbf{h}_+(t') dt'\right) = \exp(i\gamma_1 \mathbf{I}_z) \exp(i\beta_1 \mathbf{I}_y) \exp(i\alpha_1 \mathbf{I}_z) \quad (31)$$

which, along with the initial condition of equation (26), gives

$$\begin{aligned} \sigma_{11} &= \cos \beta_1, \\ \sigma_{12} &= -\sin \beta_1 e^{i\gamma_1}. \end{aligned} \quad (32)$$

Here \mathbf{I}_y and \mathbf{I}_z are spin operators for spin 1/2. Note that with this initial condition result (32) does not depend on α_1 . This fact can be used to establish the relation between the Euler angles and the Riccati equation.

To assess the response of the system to an RF pulse, following [17], we define the quantities

$$\begin{aligned} (\tilde{\mathbf{I}} \cdot \mathbf{n})_1 &= (\tilde{\mathbf{I}}^r \cdot \mathbf{n}) \cos \omega t, \\ (\tilde{\mathbf{I}} \cdot \mathbf{n})_2 &= (\tilde{\mathbf{I}}^r \cdot \mathbf{n}) \sin \omega t, \end{aligned} \quad (33)$$

where the corresponding reduced angular momentum components $\tilde{\mathbf{I}}_x$, $\tilde{\mathbf{I}}_y$ and $\tilde{\mathbf{I}}_z$ of spin 7/2 are in the representation where the quadrupolar Hamiltonian is diagonal. These can be deduced from equation (15). Transforming equation (33) into the interaction picture (equation (17)) and truncating high frequency terms results in

$$\begin{aligned} (\tilde{\mathbf{I}} \cdot \mathbf{n})_1^{\text{int}} &= \frac{1}{4} \mathbf{P}, \\ (\tilde{\mathbf{I}} \cdot \mathbf{n})_2^{\text{int}} &= \frac{1}{4} \mathbf{Q}, \end{aligned} \quad (34)$$

In the same representation as the density matrix, see equation (29), defined by the transformation \mathbf{T} of equation (22), operators \mathbf{P} and \mathbf{Q} are of the forms

$$\mathbf{P} = \begin{bmatrix} 0 & r & 0 & 0 \\ r & 0 & 0 & 0 \\ 0 & 0 & 0 & r \\ 0 & 0 & r & 0 \end{bmatrix}, \quad \mathbf{Q} = \begin{bmatrix} 0 & -ir & 0 & 0 \\ ir & 0 & 0 & 0 \\ 0 & 0 & 0 & ir \\ 0 & 0 & -ir & 0 \end{bmatrix}. \quad (35)$$

The response of the system can then be represented by the following quantities

$$\begin{aligned} W_1 &= \text{tr} \left\{ \frac{1}{4} \mathbf{P} \tilde{\rho}(t) \right\}, \\ W_2 &= \text{tr} \left\{ \frac{1}{4} \mathbf{Q} \tilde{\rho}(t) \right\}. \end{aligned} \quad (36)$$

Using the Euler angle parametrization of density matrix (32) gives

$$\begin{aligned} W_1 &= -r \sin \beta_1 \cos \gamma_1, \\ W_2 &= r \sin \beta_1 \sin \gamma_1. \end{aligned} \quad (37)$$

Ramamoorthy introduces the concept of inversion of quadrupolar systems [18]. This is defined in our notation for a quadrupole as

$$W_3 = \text{tr} \left\{ \frac{1}{4} \mathbf{R} r \tilde{\rho}(t) \right\}, \quad (38)$$

which gives

$$W_3 = r \cos \beta_1. \quad (39)$$

W_3 is inverted for $\beta_1 = \pi$. Note that the quantity W_3 does not represent the signal actually measured in NQR spectrometers.

It is clear from equations (28), (29), (32), (36) and (37) that the response of the system is determined by the sum of the two Pauli spin matrix type responses. We can thus introduce two pseudospins 1/2 to illustrate the physical picture of the evolution. The corresponding components of the associated magnetization vectors are

$$\begin{aligned} M_x^\pm &= -\sin \beta_1 \cos \gamma_1 M_0, \\ M_y^\pm &= \sin \beta_1 \sin \gamma_1 M_0, \\ M_z^\pm &= \pm \cos \beta_1 M_0, \end{aligned} \quad (40)$$

where $M_0 = r m_0$ and m_0 is the constant.

3.2. On-resonance solution and the NQR $\pi/2$ pulses

Consider now the application of the RF pulse to an on-resonance situation, i.e., $\Delta\omega = 0$. Solving the Riccati equation we obtain Euler angles of

$$\begin{aligned} \gamma_1 &= \frac{\pi}{2} - \phi, \\ \beta_1 &= \int_0^t \omega_{\text{1eff}}(t') dt'. \end{aligned} \quad (41)$$

From equation (40) we find that our system can be visualized as being composed of two pseudospins 1/2 with equal M_x and M_y components and oppositely directed M_z components. The simple magnetization trajectories on-resonance are obtained from equation (41). It is clear that when $\beta_1 = \pi/2$ these two associated magnetization vectors are aligned, thereby allowing an NQR definition of a $\pi/2$ pulse. On the other hand when $\beta_1 = \pi$ these are directed oppositely from each other and their initial direction. This situation can be considered to correspond to a π pulse. The durations of these pulses are determined by the effective frequency of the applied RF field. In the case of the single crystal the duration of a π pulse is twice that of a $\pi/2$ pulse. In the case of powders the response of the system is represented by the integration of equations (37) and (39) over polar and azimuthal angles

$$\tilde{W}_p = \iint W_p \frac{\sin \theta_L d\theta_L d\phi_L}{4\pi}, \quad (42)$$

where $p = 1, 2, 3$. The duration of the π and $\pi/2$ pulses in this situation can be determined, for example, by setting $\phi = 0$. In this case a $\pi/2$ pulse corresponds to the maximum of W_2 as a function of time whereas a π pulse corresponds to the minimum of W_2 . The application of composite and shaped pulses to such systems can be considered in a similar manner to [6, 7]. The main feature of the rectangular pulse is the extensive side band excitation beyond resonance conditions. Shaping of the pulse can produce a complete, localized and uniform excitation profile [8]. The shape of the pulse determines the excitation profile, the effective width of which is controlled by suitable pulse parameters [8, 19]. For a pulse to selectively excite a given transition it is important that the off-resonance profile of the pulse be considerably less than any neighbouring transition [19].

3.3. Comparison with corresponding spin 1/2 system

The response of the system in the laboratory frame can be found in the following manner. Transforming the density matrix of equation (29) from the interaction picture to the laboratory frame and using the Euler angle parametrization of equation (32) requires only the change

$$\gamma_1 \rightarrow \gamma_1 + \omega t. \quad (43)$$

Now we transform the density matrix of equations (28) and (29) to the basis $|1\rangle, |-3\rangle, |3\rangle$ and $|-1\rangle$ to obtain

$$\rho(t) = \mathbf{T}^+ \tilde{\rho}(t) \mathbf{T} = \begin{bmatrix} \sigma_{11} & (\alpha - i\beta)\sigma_{12}/r & \sigma_{12}\gamma/r & 0 \\ (\alpha + i\beta)\sigma_{12}^*/r & -\sigma_{11} & 0 & -\sigma_{12}^*\gamma/r \\ \sigma_{12}^*\gamma/r & 0 & -\sigma_{11} & (\alpha - i\beta)\sigma_{12}^*/r \\ 0 & -\sigma_{12}\gamma/r & (\alpha + i\beta)\sigma_{12}/r & \sigma_{11} \end{bmatrix}. \quad (44)$$

Then the response is given by

$$W = \text{Tr}\{(\tilde{\mathbf{I}} \cdot \mathbf{n})\rho(t)\} = r(\sigma_{12} + \sigma_{12}^*) \quad (45)$$

or, using equations (32) and (43),

$$W = -2r \sin \beta_1 \cos(\gamma_1 + \omega t). \quad (46)$$

The response of equation (42) is similar to the corresponding response of the spin 1/2 system in the laboratory frame. Apart from the factor $2r$ this type of response is given by spin 1/2 with the following changes

$$\omega_0 \rightarrow \omega_Q, \quad \Delta\omega \rightarrow -\Delta\omega, \quad \omega_1 \rightarrow \omega_{1\text{eff}}. \quad (47)$$

The corresponding response to equation (46) for a spin 1/2 is given by

$$W_{1/2} = \text{Tr}\{\mathbf{I}_{x1/2}\rho_{1/2}(t)\}, \quad (48)$$

where $\mathbf{I}_{x1/2}$ and $\rho_{1/2}(t)$ are the x spin 1/2 operator and the spin 1/2 density matrix in the laboratory frame, respectively. Equations (18)–(46) are general for 1/2 integral spins. For example, substituting the Euler angles and $\omega_{1\text{eff}}$ for spin 3/2 for a pulse of constant amplitude and phase [6] into equations (46) recovers equation (30) of [1].

3.4. Transitions $|\pm 4\rangle \rightarrow |\pm 2\rangle$

In order to consider the ‘double quantum’ transition $|\pm 4\rangle \rightarrow |\pm 2\rangle$, we create the reduced matrices of the form of equations (15) and (20) where now the states are $|4\rangle, |-2\rangle, |2\rangle, |-4\rangle$. The calculation of the pulse response is similar to the $|\pm 3\rangle \rightarrow |\pm 1\rangle$

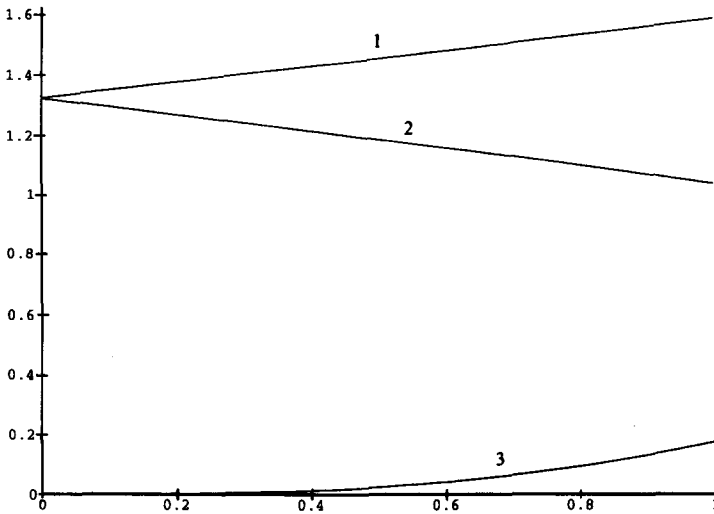


Figure 3. The values a_+ , a_- and e as functions of η for the single quantum transition $|\pm 2\rangle \rightarrow |\pm 1\rangle$: 1, a_+ ; 2, a_- ; and 3, $-e$.

transition considered above. The main difference in the result is the appearance of the different $\omega_{1\text{eff}}$ given by

$$\begin{aligned} \omega_{1\text{eff}} &= \omega_1 r, & (49) \\ r &= (\alpha^2 + \beta^2 + \gamma^2)^{1/2} \\ \alpha &= 2a_+ \sin \theta_L \cos \phi_L, \\ \beta &= 2a_- \sin \theta_L \cos \phi_L, \\ \gamma &= 2e \cos \theta_L, \end{aligned}$$

where θ_L and ϕ_L are polar and azimuthal angles specifying the orientation of the RF coil with respect to QPAS of the crystal and a different ω_Q , given by

$$\omega_Q = \frac{e^2 q Q}{84} (E_2 - E_4). \tag{50}$$

Here

$$\begin{aligned} a_{\pm} &= \pm \frac{1}{2} (7)^{1/2} U_{48} U_{22} + (3)^{1/2} U_{22} U_{46} \pm \frac{1}{2} (15)^{1/2} U_{24} U_{46} + 2U_{24} U_{44} \pm \frac{1}{2} (15)^{1/2} U_{26} U_{44} \\ &+ (3)^{1/2} U_{26} U_{42} \pm \frac{1}{2} (7)^{1/2} U_{28} U_{42}, \\ e &= \frac{5}{2} U_{22} U_{42} + \frac{1}{2} U_{24} U_{44} - \frac{3}{2} U_{26} U_{46} - \frac{7}{2} U_{28} U_{48}. \end{aligned} \tag{51}$$

For the ‘single quantum’ transitions and the ‘triple quantum’ transition the states can be included in the reduced RF and quadrupolar matrices in a similar manner in order to apply the above formulation. For example, for the ‘triple quantum’ transition, $|\pm 4\rangle \rightarrow |\pm 1\rangle$, the 4×4 matrices are given in the $|4\rangle, |1\rangle, |-1\rangle$ and $|-4\rangle$

representation. The values a_{\pm} and e required for the calculation of the effective frequency are

$$a_{\pm} = \pm \frac{1}{2} (7)^{1/2} U_{11} U_{42} \pm (3)^{1/2} U_{42} U_{13} + \frac{1}{2} (15)^{1/2} U_{44} U_{13} \pm 2 U_{44} U_{15} + \frac{1}{2} (15)^{1/2} U_{46} U_{15} \\ \pm (3)^{1/2} U_{46} U_{17} + \frac{1}{2} (7)^{1/2} U_{17} U_{48}, \\ e = \frac{7}{2} U_{11} U_{48} + \frac{3}{2} U_{13} U_{46} - \frac{1}{2} U_{15} U_{44} - \frac{5}{2} U_{17} U_{42}; \quad (52)$$

and now

$$\omega_Q = \frac{e^2 q Q}{84} (E_1 - E_4). \quad (53)$$

4. Conclusion

Note that when $\eta = 0$ all effective frequencies of multiquantum transitions vanish. For the single quantum transitions we obtain (for $\eta \neq 0$)

$$\omega_Q = \frac{e^2 q Q}{84} (E_1 - E_2), \\ a_{\pm} = \pm \frac{1}{2} (7)^{1/2} U_{11} U_{22} \pm (3)^{1/2} U_{22} U_{13} + \frac{1}{2} (15)^{1/2} U_{24} U_{13} \pm 2 U_{24} U_{15} + \frac{1}{2} (15)^{1/2} U_{26} U_{15} \\ \pm (3)^{1/2} U_{26} U_{17} + \frac{1}{2} (7)^{1/2} U_{17} U_{28}, \\ e = \frac{7}{2} U_{11} U_{28} + \frac{3}{2} U_{13} U_{26} - \frac{1}{2} U_{15} U_{24} - \frac{5}{2} U_{17} U_{22}; \quad (54)$$

These are shown in figure 3 as function of η . Comparison with figure 1 shows that in the case of double quantum transitions the effective frequencies are considerably smaller (and thus the pulses should be longer to achieve the same excitation) than in the case of single quantum transitions.

$$\omega_Q = \frac{e^2 q Q}{84} (E_2 - E_3), \\ a_{\pm} = \pm \frac{1}{2} (7)^{1/2} U_{31} U_{22} \pm (3)^{1/2} U_{22} U_{33} \pm \frac{1}{2} (15)^{1/2} U_{24} U_{33} + 2 U_{35} U_{24} \pm \frac{1}{2} (15)^{1/2} U_{35} U_{26} \\ + (3)^{1/2} U_{37} U_{26} \pm \frac{1}{2} (7)^{1/2} U_{37} U_{28}, \\ e = \frac{5}{2} U_{22} U_{37} + \frac{1}{2} U_{35} U_{24} - \frac{3}{2} U_{33} U_{26} - \frac{7}{2} U_{31} U_{28}; \quad (55)$$

$$\begin{aligned} \omega_Q &= \frac{e^2 q Q}{84} (E_3 - E_4), \\ a_{\pm} &= \pm \frac{1}{2} (7)^{1/2} U_{42} U_{31} \pm (3)^{1/2} U_{42} U_{33} + \frac{1}{2} (15)^{1/2} U_{44} U_{35} \pm 2 U_{44} U_{46} + \frac{1}{2} (15)^{1/2} U_{35} U_{46} \\ &\quad \pm (3)^{1/2} U_{46} U_{37} + \frac{1}{2} (7)^{1/2} U_{37} U_{48}, \\ e &= \frac{7}{2} U_{31} U_{48} + \frac{3}{2} U_{33} U_{46} - \frac{1}{2} U_{35} U_{44} - \frac{5}{2} U_{37} U_{42}. \end{aligned} \quad (56)$$

In the case of $\eta = 0$ expressions (54)–(56) reduce to the simple results [6]

$$\begin{aligned} \omega_Q &= \frac{3}{14} e^2 q Q, \omega_{\text{eff}} = \omega_1 (7)^{1/2} \sin \theta_L; \\ \omega_Q &= \frac{1}{7} e^2 q Q, \omega_{\text{eff}} = \omega_1 (12)^{1/2} \sin \theta_L; \\ \omega_Q &= \frac{1}{14} e^2 q Q, \omega_{\text{eff}} = \omega_1 (15)^{1/2} \sin \theta_L. \end{aligned}$$

The results of the paper are impossible to obtain without the aid of computer algebra. Even with computer algebra it is necessary to organize the treatment in a way that leads to a curtailment of the long and unmanageable expressions that can occur. This was not a trivial task and extensions to the higher spin cases is not routine.

The results here are practical and easily programmable to give numerical results in special cases. We checked our analytical results for each transition numerically using the ‘Maple’ built in routine for the numerical solution of eigenfunction–eigenvalue problems, an example of which is given in the appendix. Moreover, using similar techniques, it is straightforward to modify initial conditions (26) to include other cases. Hence, a sequence of pulses can be treated in NQR for spin 7/2.

Finally, we have been able to provide a definition and some understanding of $\pi/2$ and π pulses in NQR. The physical interpretation is different from NMR, which is based upon a vector, in that NQR requires two vectors which can be parallel or antiparallel to produce a $\pi/2$ and a π pulse, respectively. The length of these pulses depends upon which transitions are being excited.

Appendix

```
#####
```

This Maple program numerically calculates matrix forms of spin components in the representation where the quadrupolar Hamiltonian is diagonal for arbitrary η .

```
#####
```

```
#set the number of digits to 15 and spin magnitude to 7/2
Digits:=15;
i:=7/2;
# the next seventeen lines are used to calculate spin components
#  $I_x, I_y, I_z$  and  $i_q = i(i+1) - 3i_z^2$  in  $|I, M\rangle$  basis
nsize:=2*i+1;
i_plus:=array(sparse,1..nsize,1..nsize); i_minus:=array(1..nsize,1..nsize);
i_x:=array(1..nsize,1..nsize);
i_y:=array(1..nsize,1..nsize); i_z:=array(sparse,1..nsize,1..nsize);
i_q:=array(sparse,1..nsize,1..nsize);
i_row:=1;
for m from -i to i-1 do
  i_plus[i_row,i_row+1]:=evalf(sqrt((i+m+1)*(i-m)));
  i_q[i_row,i_row]:=i*(i+1)-3*m**2;
  i_z[i_row,i_row]:=-m;
  i_row:=i_row+1;
od;
i_z[i_row,i_row]:=-i;
i_q[i_row,i_row]:=i*(i+1)-3*i**2;
i_minus:=evalm(transpose(i_plus));
i_x:=evalm(i_plus+i_minus)/2;
i_y:=evalm((i_plus-i_minus)/(2*I));

#set  $\eta = 0.385$  and calculate  $H_Q$  (units of  $\hbar^2 qQ / 84$ )
eta:=0.385;
i_qeta:=evalm(-i_q+eta/2*(i_plus*i_plus+i_minus*i_minus));
# solve eigenvalue and eigenfunction problem for  $H_Q$  and assign the matrix
# containing eigenfunctions to T. Note that Maple arranges eigenvalues from lowest
# to highest and columns of T contain corresponding eigenfunctions.
evalf(Eigenvals(i_qeta,vecs));
T:=evalm(vecs);
t1:=transpose(T);
# calculate spin components and quadrupolar Hamiltonian in the representation
# where the quadrupolar Hamiltonian is diagonal
i_xnew:=evalm(t1&*i_x&*T);
i_ynew:=evalm(t1&*i_y&*T);
i_znew:=evalm(t1&*i_z&*T);
i_qetane:=evalm(t1&*i_qeta&*T);
```

References

- [1] PRATT, J. C., 1977, *Molec. Phys.*, **49**, 539.
- [2] VEGA, S., 1978, *J. chem. Phys.*, **68**, 5518.
- [3] RAMAMOORTHY, A., and NARASIMHAN, P. T., 1991, *Molec. Phys.*, **73**, 207.
- [4] ZUEVA, O. S., and KESSEL, A. R., 1977, *Sov. Phys. JETP*, **46**, 1136.
- [5] KRISHNAN, M. S., TEMME, F., and SANCTUARY, B. C., 1993, *Molec. Phys.*, **78**, 1385.
- [6] AGEEV, S. Z., ISBISTER, D. J., and SANCTUARY, B. C., 1994, *Molec. Phys.*, **83**, 193.

- [7] AGEEV, S. Z., and SANCTUARY, B. C., 1994, *Chem. Phys. Lett.*, **225**, 499.
- [8] WARREN, W. S., and SILVER, M. S., 1988, *Adv. magn. Reson.*, **12**, 247; McDONALD, S., and WARREN, W. S., 1991, *Concepts magn. Reson.*, **3**, 55.
- [9] CHAR, B. W., GEDDES, K. O., GONNET, G. H., LEONG, B. L., MONAGEN, M. B., and WATT, S. M., 1993, *Maple V, Language Reference Manual; Maple V Library Reference Manual* (Berlin: Springer-Verlag).
- [10] RAMAMOORTHY, A., 1991, *Molec. Phys.*, **72**, 1425.
- [11] HATANAKA, H., TERAOKA, T., and HASHI, T., 1975, *J. phys. Soc. Jap.* **39**, 835; HATANAKA, H., and HASHI, T., 1975, *J. phys. Soc. Jap.*, **39**, 1139.
- [12] REDDY, R., and HARASIMHAN, P. T., 1988, *J. molec. Struct.*, **192**, 309.
- [13] BLOCH, F., and SIEGERT, A., 1940, *Phys. Rev.*, **57**, 222; FURMAN, G. B., 1990, *Z. Natur.*, **45a**, 565.
- [14] CREEL, R. B., 1983, *J. magn. Reson.*, **52**, 515.
- [15] WOKAUN, A., and ERNST, R. R., 1977, *J. chem. Phys.*, **67**, 1977.
- [16] ZHOU, J., GAO, H., and SANCTUARY, B. C., 1993, *J. magn. Reson. A*, **102**, 137; ZHOU, J., YE, C., and SANCTUARY, B. C., 1994, *J. chem. Phys.*, **101**, 6424.
- [17] HÄBERLEN, U., 1976, *High Resolution NMR in Solids: Selective Averaging* (New York: Academic Press).
- [18] RAMAMOORTHY, A., CHANDRAKUMAR, N., DUBEY, A. K., and NARASIMHAN, P. T., 1993, *J. magn. Reson. A*, **102**, 274.
- [19] GAGGELI, E., and VALENSIN, G., 1992, *Concepts magn. Reson.*, **4**, 339 and references therein.